Paleomagnetic study of the Chicxulub impact breccia sequence in the Santa Elena borehole—evidence of reverse polarity remanent magnetizations

Estudio paleomagnético de la secuencia de brechas de impacto de Chicxulub en el pozo Santa Elena—evidencia de magnetizaciones de polaridad reversa remanentes

Miriam **Velasco-Villarreal**[1,*], Ligia **Pérez-Cruz**[1,2,3], Jaime **Urrutia-Fucugauchi**[1,2]

[1] Proyecto Universitario de Perforaciones en Océanos y Continentes, Instituto de Geofísica. Universidad Nacional Autónoma de México, Coyoacán 04510 México

[2] Instituto de Investigación Científica y Estudios Avanzados Chicxulub, Parque Científico y Tecnológico de Yucatán, Sierra Papacal, Mérida, Yucatán 97302, México

[3] Coordinación de Plataformas Oceanográficas, Coordinación de la Investigación Científica, Universidad Nacional Autónoma de México, Coyoacán 04510, México

* Corresponding author:
(M. Velasco-Villareal) *miriam@geofisica.unam.mx*

How to cite this article:
Velasco-Villarreal, M., Pérez-Cruz, L., Urrutia-Fucugauchi, J., 2024, Paleomagnetic study of the Chicxulub impact breccia sequence in the Santa Elena borehole—evidence of reverse polarity remanent magnetizations: Boletín de la Sociedad Geológica Mexicana, 76 (3), A130224 http://dx.doi.org/10.18268/BSGM2024v76n3a130224

Manuscript received: October 19, 2023
Corrected manuscript received: February 1, 2024
Manuscript accepted: February 13, 2024

Peer Reviewing under the responsibility of Universidad Nacional Autónoma de México.

ABSTRACT

Results of a paleomagnetic study of the Chicxulub breccias in the Santa Elena borehole are presented. The impact produced a deep excavation in the Yucatan platform, with fragmentation and deformation of the target lithologies. Fragmented material was ejected at high velocities and high temperatures, forming a central plume and lateral curtains. In the target zone, crustal rocks were melted forming a melt pool with breccias emplaced in the crater and proximal areas. Here we analyze the impact ejecta in a proximal location, south of the crater rim at 110 km away from the crater center at Chicxulub Puerto. The breccias in the Santa Elena borehole cored between 332 and 504 m depth are formed by melt, basement and carbonate clasts within carbonate-rich and melt-basement-rich matrix. The magnetic susceptibility, remanent magnetization and coercivity and unblocking temperature spectra provide constraints on the breccia emplacement. Thermal and alternating field demagnetization shows univectorial and two-component magnetizations with upward inclinations and only three samples with downward inclinations. Paleomagnetic studies of the impact breccias have shown mixed normal and reverse polarities, which have been interpreted in terms of reverse polarity characteristic magnetizations and hydrothermally induced overprints that vary with relative location. The upward paleomagnetic inclinations in the Santa Elena breccia section are consistent with reverse polarity magnetizations acquired during the ch29r chron.

Keywords: Chicxulub crater, impact breccias, paleomagnetism, magnetic polarity, emplacement mode, hydrothermal system

RESUMEN

Se presentan los resultados del estudio paleomagnético de las brechas de impacto en el pozo Santa Elena. El impacto produjo una excavación profunda en la plataforma de Yucatán, con fragmentación y deformación. El material fragmentado fue expulsado a altas velocidades y altas temperaturas, formando una pluma central y cortinas laterales. En la zona de impacto, las rocas de la corteza se fragmentaron y fundieron, con brechas emplazadas en el cráter y las áreas próximas. En este estudio, analizamos la secuencia de brechas de impacto en el pozo Santa Elena, ubicado a ~110 km del centro del cráter en Chicxulub Puerto. La secuencia de brechas está entre 332 y 504 m de profundidad, formada por clastos de fusión, basamento y carbonatos dentro de una matriz rica en carbonatos o en basamento y roca fundida. Se analizan datos de susceptibilidad magnética, magnetización remanente y los espectros de temperatura y de coercitividad. La desmagnetización térmica y de campos alternos muestra magnetizaciones univectoriales y de dos componentes, con inclinaciones arriba de la horizontal, con tres muestras con inclinaciones debajo de la horizontal. Estudios paleomagnéticos en las brechas de impacto han mostrado polaridades normales e inversas mixtas, que se han interpretado en términos de magnetizaciones de polaridad reversa y magnetizaciones secundarias, generadas por alteración hidrotermal. Los efectos de alteración hidrotermal varían con la distancia respecto a la zona central del cráter. Las inclinaciones paleomagnéticas negativas en la sección de la brecha de Santa Elena se interpretan como magnetizaciones de polaridad reversa, consistente con el cron ch29r de polaridad reversa.

Palabras Cráter Chicxulub, brechas de impacto, paleomagnetismo, polaridad magnética, modo de emplazamiento, sistema hidrotermal

http://dx.doi.org/10.18268/BSGM2024v76n3a130224

1. Introduction

The Chicxulub crater was formed by an asteroid impact ~66 Ma ago at the Cretaceous/Paleogene (K/Pg) boundary. The crater has a 200 km rim diameter located in the northwestern sector of the Yucatan peninsula, with center in Chicxulub Puerto in the coastline (Figure 1). In the target area, fragmented material was ejected at high velocities and high temperatures, forming a central plume and lateral curtains. The impact ejecta had a global distribution, with fine grained material reaching the stratosphere and blocking the solar radiation. The impact affected the life support systems, resulting in the extinction of 76 % of species in the continents and oceans (Alvarez *et al.*, 1980; Schulte *et al.*, 2010).

As part of the oil exploration programs in southern Mexico, geophysical surveys documented a large semicircular gravity anomaly in the northern Yucatan peninsula (Cornejo-Toledo and Hernandez-Osuna, 1950). Drilling found an igneous-textured unit and the structure was interpreted as a large volcanic center of Late Cretaceous age (Lopez Ramos, 1975). In the 1970's an aeromagnetic survey documented a high amplitude anomaly within the center of the gravity anomaly, which Penfield and Camargo-Zanoguera (1981) interpreted as an impact crater.

The report of a large crater generated interest in relation to the Alvarez *et al.* (1980) impact theory for the K/Pg boundary mass extinction. Several years later search for the K/Pg impact site focused

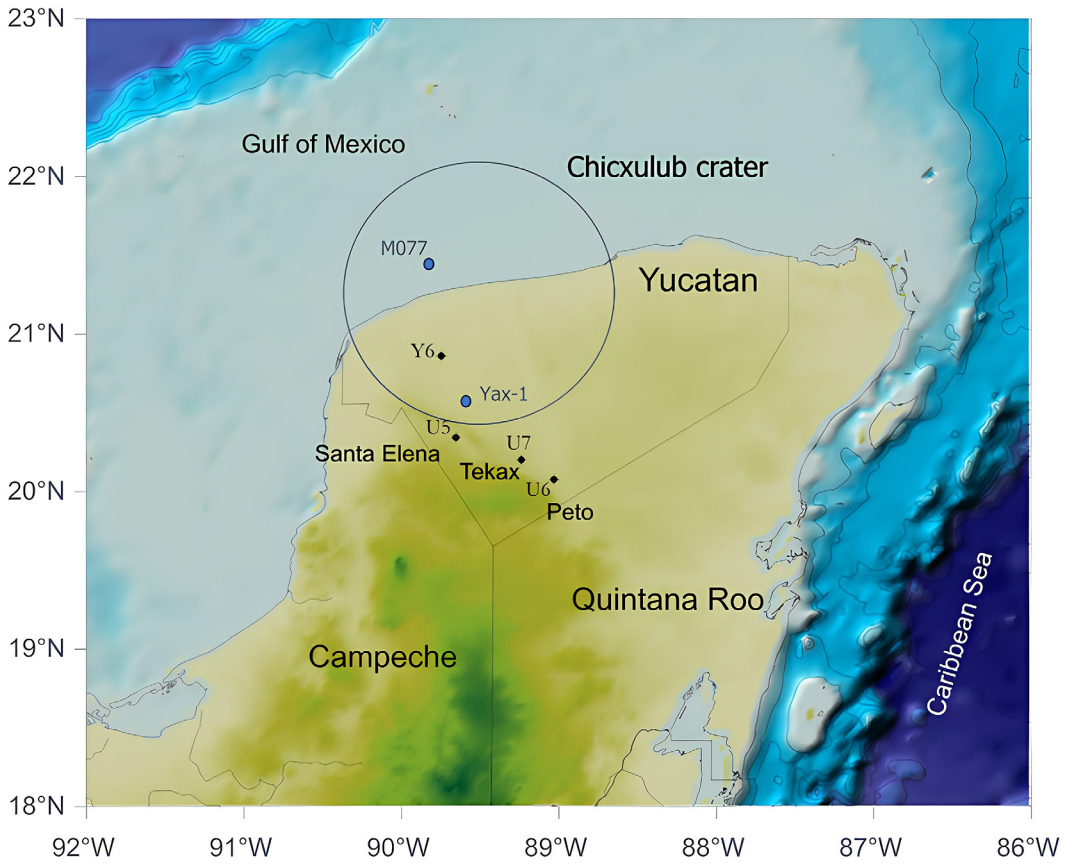

Figure 1 (a) Location of Chicxulub impact crater in Yucatan peninsula. The location of the Santa Elena borehole is indicated. The two other boreholes that intercepted impact breccias are Peto (U6) and Tekax (U7) boreholes. Locations of Yucatan 6 Y6 in the central crater sector and M0077A over the peak ring in the marine sector are also indicated.

http://dx.doi.org/10.18268/BSGM2024v76n3a130224

on the Gulf of Mexico-Caribbean Sea (Bourgeois *et al.*, 1988), which led to revising the oil exploration data. Hildebrand *et al.* (1991) proposed that the Chicxulub structure was the K/Pg boundary impact site, with the igneous-textured rocks interpreted as impact melt and breccias formed by the impact. Radiometric studies on melt and melt-rich breccias from the Yucatan-6 and Chicxulub-1 cores reported dates coinciding with the K/Pg boundary (Sharpton *et al.*, 1992).

Paleomagnetic studies on Chicxulub impactites showed reverse polarity magnetizations in cores from the Yucatan-6 and Chicxulub-1 boreholes, consistent with the expected reverse polarity for ch29r chron (Sharpton *et al.*, 1992; Urrutia-Fucugauchi *et al.*, 1994). Paleomagnetic studies of the impact breccias cored in subsequent drilling programs in the Chicxulub crater reported mixed reverse and normal polarity magnetizations for the breccia sequence (*e.g.*, Steiner, 1996; Urrutia-Fucugauchi *et al.*, 2004). The secondary magnetizations have been interpreted in terms of remagnetizations associated with an extended magnetization acquisition interval and hydrothermal alteration (Pilkington *et al.*, 2004; Velasco-Villarreal *et al.*, 2011; Kring *et al.*, 2020).

Impact cratering involves conditions of high energy and extreme pressures and temperatures, with deformation and fragmentation of target material (Melosh, 1989; Pierazzo and Melosh, 2000; Collins *et al.*, 2008; Urrutia-Fucugauchi and Pérez-Cruz, 2009). Impact ejecta formed by mixtures of fragmented, melted and vaporized target and bolide material. Collapse of the ejecta plume results in crater fill deposits and adjacent proximal deposits, which record the ejecta emplacement and conditions. The high temperatures formed a thick melt sheet and a long-lived hydrothermal system (Kring *et al.*, 2020). The high temperatures, shock effects and hydrothermal fluids affect the magnetic mineralogy.

Paleomagnetic studies have proved well suited for providing constraints on age, impact effects and post-impact alteration (*e.g.*, Halls, 1979; Urrutia-Fucugauchi *et al.*, 1994; Urrutia-Fucugauchi *et al.*, 2004; Elmore and Dulin, 2007; Louzada *et al.*, 2008; Pohl *et al.*, 2010; Yokoyama *et al.*, 2012; Fairchild *et al.*, 2016). The accuracy and reliability in paleomagnetic studies of impact structures and shocked lithologies depend on the remagnetization effects, with the primary and secondary magnetization isolated. The impact breccias are characterized by diverse mineralogical arrangements of clasts and matrix, shock effects, different textures and alteration processes, which are reflected in the paleomagnetic record.

Here we present results of a paleomagnetic study of the impactite section in the Santa Elena borehole (Figure 1), further examining the magnetostratigraphy and implications on emplacement and hydrothermal system.

1.1. CHICXULUB CRATER AND SANTA ELENA BOREHOLE

Chicxulub formed by an asteroid impact on the Yucatan platform, in the southern Gulf of Mexico. The crater has a multiring morphology with a peak ring (Hildebrand *et al.*, 1991; Sharpton *et al.*, 1993; Urrutia-Fucugauchi *et al.*, 2011; Gulick *et al.*, 2013; Morgan *et al.*, 2016). The impact affected the life support systems, resulting in the extinction of 76 % of species in continents and oceans and marking the Cretaceous/Paleogene boundary (Alvarez *et al.*, 1980; Schulte *et al.*, 2010). The impact involved high energy conditions, with extreme pressures and temperatures and deformation and fragmentation of target material (Melosh, 1989; Pierazzo and Melosh, 2000; Collins *et al.*, 2008).

The ejecta formed by dynamic mixtures of fragmented, melted and vaporized target and bolide material (Navarro *et al.*, 2020; Navarro *et al.*, 2021). Collapse of the ejecta plume resulted in crater fill deposits and adjacent proximal deposits that record the ejecta emplacement and conditions. The K/Pg boundary sites are marked by distinct ejecta characteristics related to distance from Chicxulub crater: (1) very proximal, (2) proximal, (3) intermediate and (4) distal sites (Schulte *et al.*, 2010). The very proximal sites up to 500 km away

http://dx.doi.org/10.18268/BSGM2024v76n3a130224

from the impact site show thick ejecta deposits. Distal sites are characterized by a few centimeters thick double layer ejecta, with a basal spherulite layer and a fine-grained clay layer (Alvarez *et al.*, 1980; Schulte *et al.*, 2010).

Within and around the crater, drill boreholes show impactite sequences up to several hundred meters thick. The breccias show an inverted stratigraphy with the basement and melt rich breccias above the carbonate rich breccias (Urrutia-Fucugauchi *et al.*, 1996). The K/Pg sections around the Gulf of Mexico Caribbean Sea region show ejecta deposits several meters thick, with high energy debris flows and tsunami deposits emplaced between the basal spherulitic layer and the clay layer (Schulte *et al.*, 2010).

The aeromagnetic studies over the central sector of crater show a high amplitude dipolar anomaly of reverse polarity with high frequency small amplitude anomalies (Penfield and Camargo-Zanoguera, 1981; Hildebrand *et al.*, 1991; Hildebrand *et al.*, 1998; Ortiz-Aleman and Urrutia-Fucugauchi, 2010). The central dipolar anomaly is associated with the basement uplift, with contributions of the melt and impact breccias. The small anomalies are likely associated with the melt and impact breccias, with contributions from crater structures involving basement units. The magnetic anomalies are constrained within the zone of high amplitude gravity anomalies, within the annular trough. Joint models of the aeromagnetic and gravity anomalies characterize the crater structures and the crater units. Constraining the sources of the magnetic anomalies requires fur-

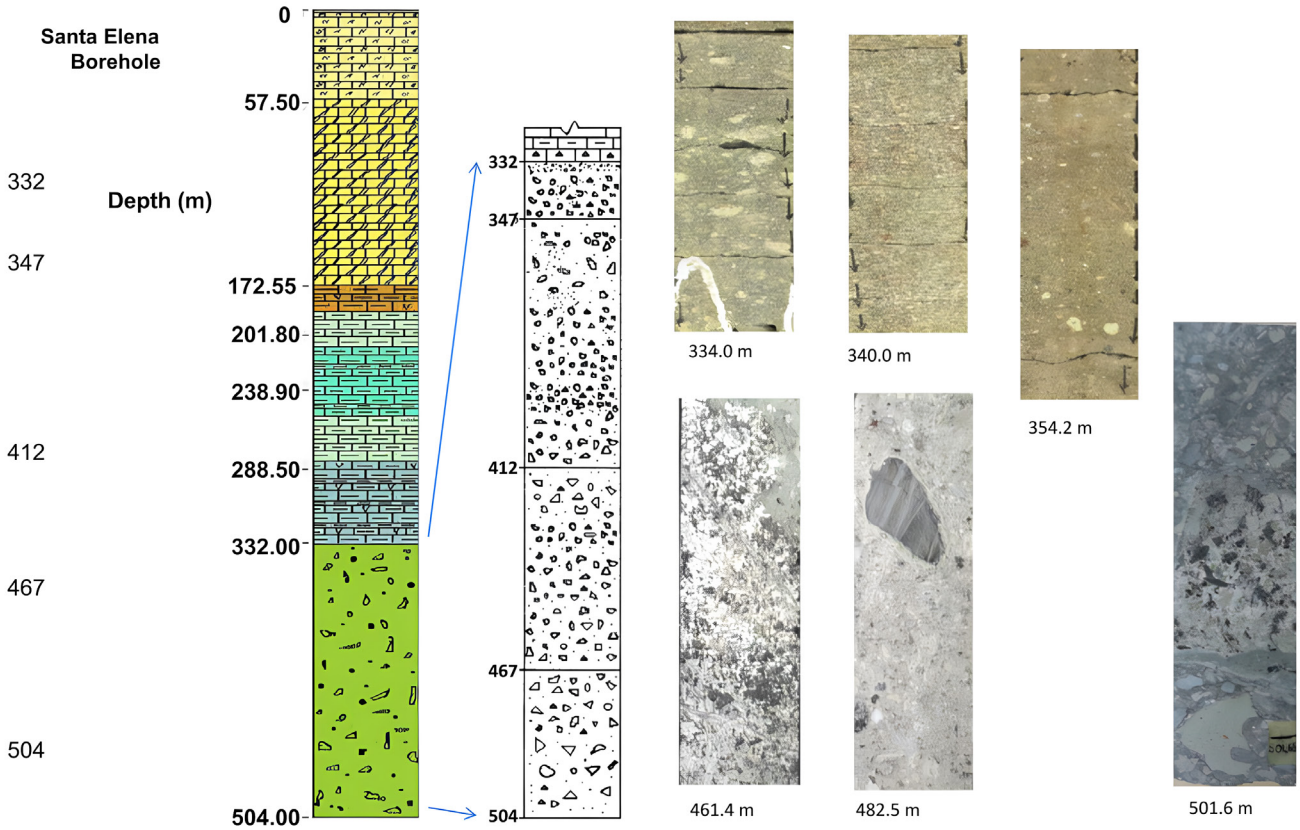

Figure 2 **Lithologic column for the Santa Elena borehole and the impact breccia section with the breccia units drilled in the 332 to 504 m depth range. Core images at different intervals through the section are included.**

http://dx.doi.org/10.18268/BSGM2024v76n3a130224

ther data on the physical property contrasts with depth, associated with the basement uplift, breccias and melt (Pilkington and Hildebrand, 2000; Urrutia-Fucugauchi *et al.*, 2022).

The Santa Elena drilling site is in the southern sector of Ticul Sierra about 3.5 km northwest of Santa Elena town at 20.34° N, 89.66° W (Urrutia-Fucugauchi *et al.*, 1996; Urrutia-Fucugauchi *et al.*, 2014). The radial distance is 110 km from Chicxulub Puerto (Figure 1). The drilling included a continuous core recovery program, providing core samples from the post-impact carbonates and the impactite section (Figure 2).

The post-impact sequence consists in about 1 m of calcareous soils, followed by 56.5 m of crystalline limestones, then 145 m of dolomitized limestones, 15 m of cream-white argillaceous fractured limestones, 115 m of argillaceous limestones with lutite beds partly affected by dolomitization and dissolution, 114 m of cream-white argillaceous limestones with lutite intercalations, and 45.5 m of limestones and lutites with evaporites.

The drilling sampled 172 m of impact breccia. The impact breccia begins from 332 to 504 m in depth and has been defined as a suevite polymictic breccia with clay-silty matrix, rich in carbonate clasts, impact glass, impact melting rock and granite clasts of the basement (Figure 2). Breccia units have been defined from analyses of matrix and clasts, with the lithological, textural and mineralogical changes, clasts and matrix (Escobar-Sánchez, 2002; Urrutia-Fucugauchi *et al.*, 2014). Subunits are marked, based on the magnetic susceptibility and magnetization intensity logs (Figure 2).

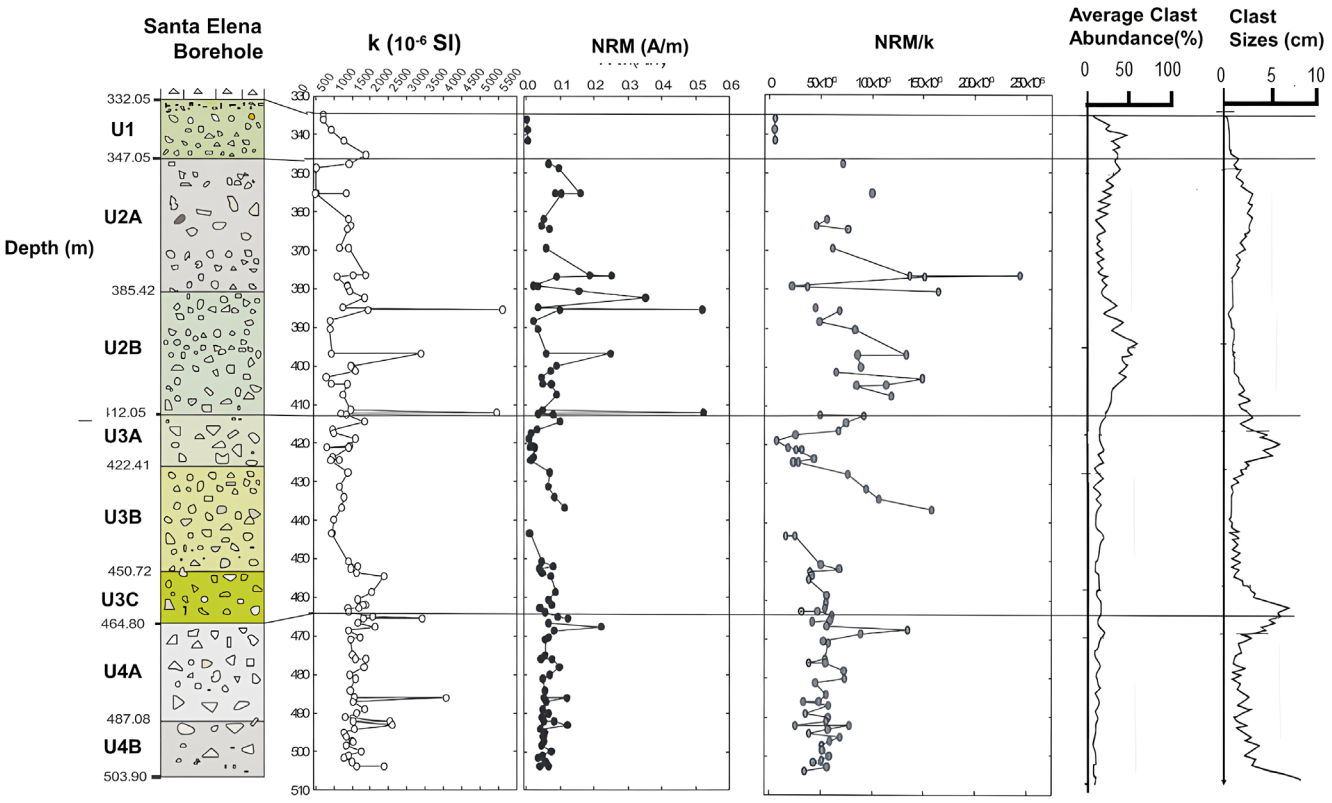

Figure 3 Logs of magnetic susceptibility, NRM intensity, NRM intensity-magnetic susceptibility ratios (this study) and average clast abundance (%) and clast sizes (cm) (Escobar Sánchez, 2002; Urrutia-Fucugauchi *et al.*, 2014). The impactite sequence is formed by four units and seven subunits (see text for description).

http://dx.doi.org/10.18268/BSGM2024v76n3a130224

2. Methods

For the study, samples were cut from the cores that were not azimuthally oriented. The declinations are referred to orientation chosen for the core segments. Part of the samples are cubes and part are cylinders.

The magnetic susceptibility was measured with a Bartington MS2 susceptibilimeter with a dual frequency sensor (Dearing, 1999). The intensity and direction of natural remanent magnetization (NRM) were measured with a JR6-A spinner magnetometer. Demagnetization by alternating fields (AF) was done with a Molspin Limited shielded demagnetizer NE2 2HE, in steps up to 100 mT at 180Hz. For thermal demagnetization, a Schonstedt TSD-1 furnace with a special metal shield was used, with a capacity of 16 samples. It has two chambers, one for heating and one for cooling. For AF demagnetization, 14 cylindrical samples (~2cm high by 2.4cm diameter) were selected. For thermal demagnetization 15 cubic samples (~ 8cm^3) were used.

For the analysis of vector components and calculation of characteristic magnetizations (ChNRM), vector plots, end point analysis and principal component analysis (PCA) were used (Zijderveld, 1967; Kirschvink, 1980; Dunlop, 1979).

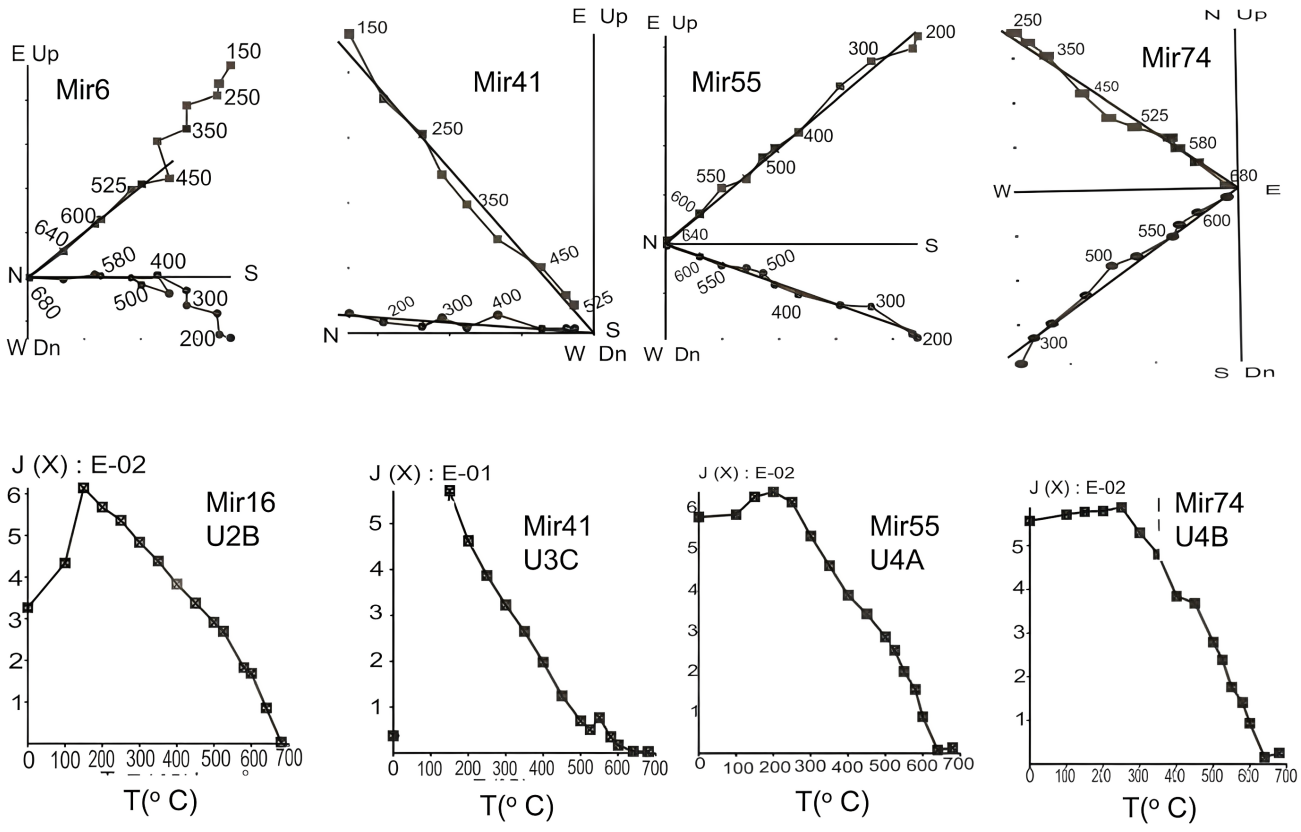

Figure 4 Vector demagnetization plots and intensity diagrams for samples with thermal demagnetization. The horizontal component is indicated by circles and the vertical component by squares. Samples from upper section units U2 to U3B, with one to two components. Samples from lower section U3C and U4 units with univectorial magnetizations Observe the similarity of unblocking temperature spectra for different units.

http://dx.doi.org/10.18268/BSGM2024v76n3a130224

3. Results

The impactite sequence is divided into four units and seven subunits (see text for description). Both parameters have similar behavior and allow the column to be divided in two parts. A lower section from 450m to ~504m depth and upper section from 332m to ~450m of depth. Average clast abundance (%) and clast sizes show a correlation with the magnetic susceptibility and magnetization intensity.

The measurements of the magnetic susceptibility and NRM intensity, as well as the size of the clasts and their abundance as a function of depth are plotted in Figure 3. Magnetic susceptibility varies from 5 to 2000 10^{-6} SI, with some high values > 5000 10-6 SI.

The ratios of NRM and magnetic susceptibility show variable behavior in the upper section with higher values than in the lower section. The clast sizes and average abundance (%) depending on the depth show that 50% of the clasts are in the lower part of unit U2A and upper part of unit U2B; while the large clast sizes are in U3A and U3B units (Figure 3).

Demagnetization vector plots and intensity diagrams for thermal demagnetization are shown in Figure 4. Vector plots show one characteristic component defined from 500°C The demagnetization for U2 shows unblocking temperatures for secondary components between 450°C and 525°C and inflexion point between 550o-580°C. In the samples from U3A and U3B units show an increment of the magnetization intensity and starts in 150°C. The vector plots show one to three secondary components. The characteristic vector

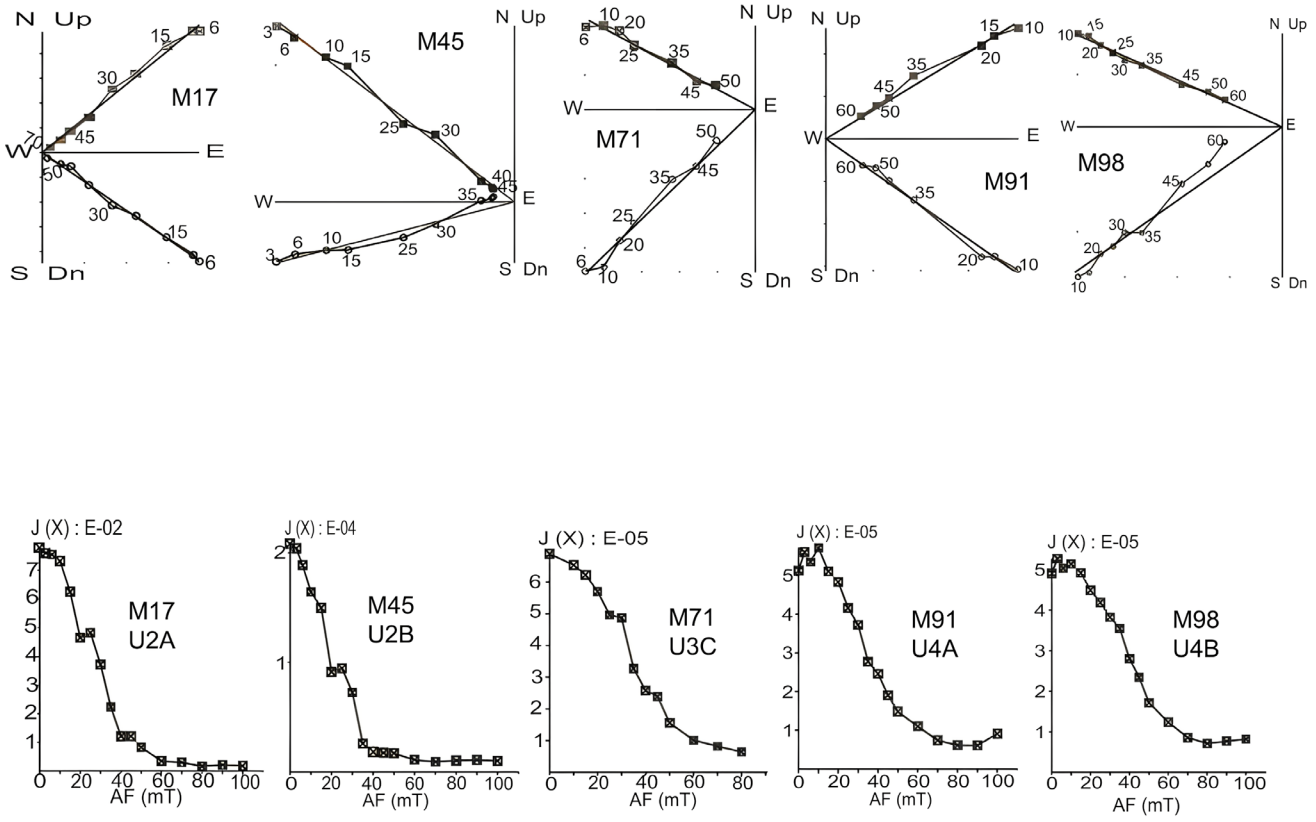

Figure 5 Vector demagnetization plots and intensity diagrams for samples of upper section with alternating field demagnetization. The horizontal component is indicated by circles and the vertical component by squares.

http://dx.doi.org/10.18268/BSGM2024v76n3a130224

is determined in the 450o-500°C range. For U3C Mir41, U4A Mir55 and U4B Mir74, vector plots show one to three components like Mir41 with a characteristic component defined >550°C. Vector plots show a magnetization change at 650-680°C suggesting a new magnetic phase, with a characteristic component defined from 200°C.

AF demagnetization shows univectorial components, with some samples showing two or three components (Figure 5). Vector plots show magnetization components isolated between 30 and 50 mT, some up to 70 mT. The intensity diagrams show an inflexion point in 40-45 mT, with some showing an increase above 80-90 mT.

Vector plots and principal component analysis were used to determine the magnetization components from thermal and AF demagnetization. Cores are not azimuthally oriented, and the inclination is used for the discussion. The results show dominantly upward magnetic inclinations, with few downward inclinations, consistent with reverse polarity magnetizations acquired in ch29r chron.

4. Discussion

The K/Pg boundary sites record distinct ejecta deposits related with the distance from Chicxulub crater: 1) very proximal sites, 2) proximal sites, 3) intermediate sites and 4) distal sites (Schulte et al,

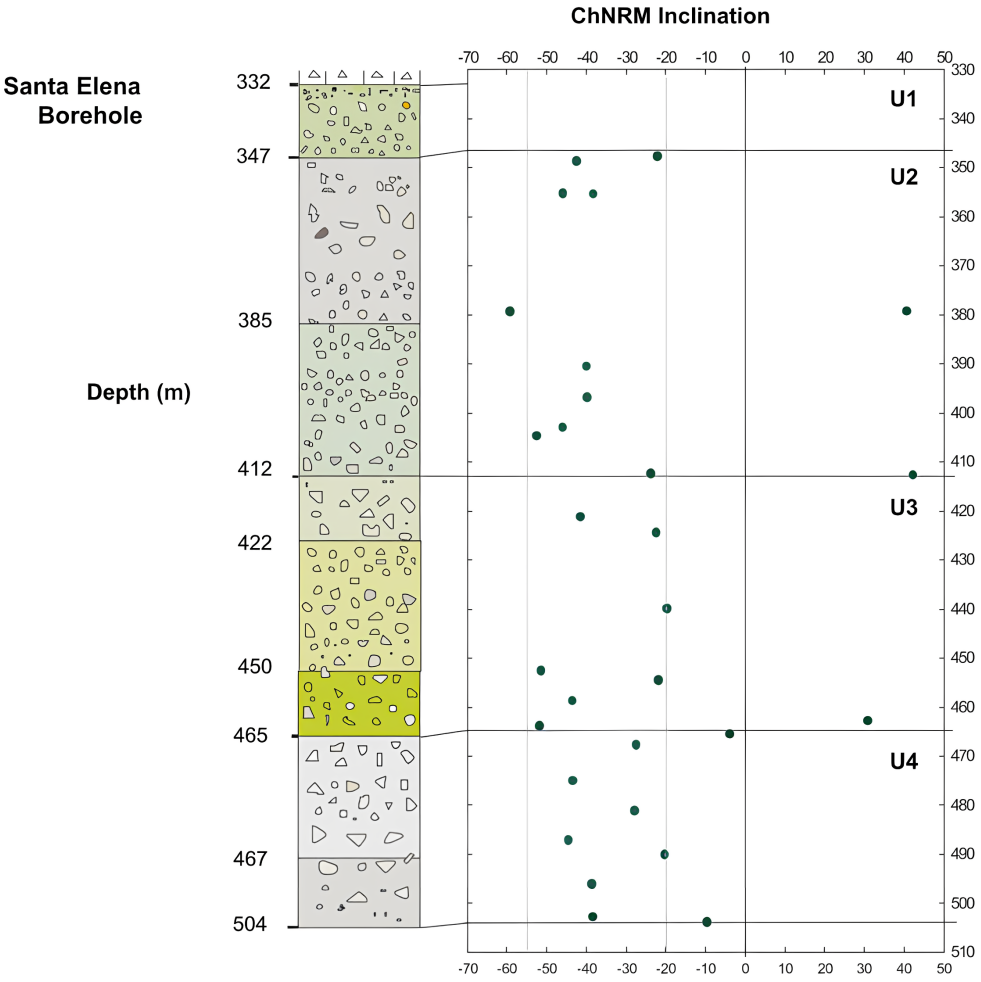

Figure 6 Plot of characteristic remanent inclination after AF and thermal demagnetization for samples of the impactite sequence. ChRM inclinations are plotted as a function of stratigraphic position through the sequence. Upward inclinations fall in the range -20° to -55°.

http://dx.doi.org/10.18268/BSGM2024v76n3a130224

2010). Paleomagnetic studies of the K/Pg boundary intermediate and distal sections have documented a magnetostratigraphy consistent with the impact occurring during reverse polarity ch29r chron. The boundary sections at proximal sites in the circum-Gulf of Mexico and Caribbean Sea show complex stratigraphy, associated with high energy debris flows and tsunami deposits. Sections at or close to the crater that include the breccia sequences are in addition affected by post-impact processes and hydrothermal alteration.

During thermal vector demagnetization, orthogonal projections show one to two components in most samples (Figure 4). The characteristic vector is well defined in samples from units U2 to U3. The samples in units U3C to U4 present a single component from almost the start of demagnetization up to 525 °C, and up to 680 °C in others. The magnetization graphs show an increase to 200-250 °C and on some samples at 350 °C and 525° C. Samples Mir16 and Mir 41 show large changes at low unblocking temperatures, indicating removal of a secondary component. An inflection is noted defining the characteristic vector in unit 2 and unit 3 samples. Unit 4 samples show small increases in Mir55 or none in Mir74. The inflection at 450-500° C suggests removal of secondary components.

During alternating field demagnetization, the orthogonal projections (Figure 5) show single component magnetizations. In some cases, there is a secondary component removed in low fields 3 to 10-15 mT, observed in U4 and in samples of U3C. A secondary component removed between 20 and 45 mT indicates intermediate components. The characteristic component shows linear trajectories; in some cases, a single vector component from the beginning to 90 mT, and some from 10 to 50 or 70 mT. In some cases, vector components deviate from the origin (M64, M98) coercivity suggesting remagnetization during treatment or incomplete separation. Secondary components of high and intermediate coercivity are observed in U2 and U3B.

Principal component analysis on the demagnetization data was used to define the characteristic inclinations, which are plotted referred to stratigraphic position (Figure 6). The magnetostratigraphic results show mainly negative inclinations, between -20 ° and -55 ° with an average inclination of -31.12°. This contrasts with the paleomagnetic results for the Yaxcopoil-1 breccia sequence, where upward and downward magnetic inclinations are recorded (Urrutia-Fucugauchi *et al.*, 2004; Velasco-Villarreal *et al.*, 2011).

Paleomagnetic analysis of impact melt rocks from Yucatan-6 borehole recorded a characteristic inclination of -42.6 ° ± 2.4°, interpreted as reverse polarity (Urrutia-Fucugauchi *et al.*, 1994). The inclination of the geomagnetic field at the Chicxulub site in northern Yucatan during the late Cretaceous was -43 ° (Besse and Courtillot, 1991; Gordon and Van der Voo, 1995). The average inclination of the characteristic NRM magnetizations of -40° to -45 ° in Yucatan-6 breccias and melt are consistent with reverse polarity (Urrutia-Fucugauchi *et al.*, 1994). The $^{40}Ar/^{39}Ar$ dating in Yucatan-6 melt samples gave an estimated crystallization age of 65.2 ± 0.4 (Sharpton *et al.*, 1992).

Magnetostratigraphic studies of the basal carbonate sequence and upper breccias drilled in the Santa Elena, Peto and Tekax boreholes are consistent with the impact occurring at the reverse ch29r chron (Rebolledo-Vieyra and Urrutia-Fucugauchi, 2006). Radiometric and stratigraphic studies by Renne *et al.* (2013) provide an age around ~66 Ma. The magnetic polarity time scale has been revised, which provides additional constraints on the chronology for ch29r chron (Ogg, 2020). The upward inclinations of samples throughout the section indicate that the ejecta acquired its magnetization during emplacement at high temperatures in a reverse polarity field.

In the lower U3C to U4 units, upward inclinations in univectorial components in the high temperature range of 525° C and 680 °C and alternating fields of 10 to 50-70mT are observed.

Large clast sizes, angular shapes and lower abundance, in addition to melt-rich matrix, suggest turbulent flow conditions for the deepest section U3C

http://dx.doi.org/10.18268/BSGM2024v76n3a130224

and U4 units, but less than those in Yaxcopoil-1. In Yaxcopoil-1, the basal surges suggest collapse of the ejecta plume under turbulent conditions as proposed by Wittmann *et al.* (2007) with data on the particle shapes, lack of particle selection and their random orientations. For the Yax U3 or US units considered as a fallback ejecta a temperature gradient towards the top is indicated. The deposit for Yax U1 and U2 units, suggests less turbulence, indicated by clast selection (Wittmann *et al.*, 2007).

The vector diagrams for thermal demagnetization of samples from the upper section U2 to U3B units show single to two component magnetizations, with characteristic components. Some samples show inflection points, in 350°C and 525 °C. The AF demagnetization vector diagrams show one or two components of medium coercivity between 20 and 45mT and high coercivity from 50 to 70mT.I In some cases the component deviates from origin indicating remagnetization o incomplete separation of high coercivity components.

The upper section shows zones with fewer clasts but large sizes such as the upper part of the unit U2A, lower part of units U2B, unit U3A, and lower part of the U3B. Zones with small size clasts are the lower part of the unit U2A and upper part U2B and U3B. U3B-U2 units may have been deposited in less turbulent environmental conditions and temperatures, which correspond with the fallback suevites drilled in the Yaxcopoil-1 borehole. The U1 appears similar to the USS and LSS units from Yaxcopoil-1 borehole, interpreted as late fall back breccias, but more studies are needed.

Pilkington *et al.* (2004) reported that Fe-oxide phases comprising limonite-goethite, magnetite, and Fe-Ti oxides occur in the impactite section of Yaxcopoil-1. Magnetite, Fe-oxyhydroxides and Fe-Ti oxides are secondary minerals in the matrix, in addition of microlites, diopside, and plagioclase, vesicles associated with quartz and clay minerals, and veins with K-feldspars and albite. Planar deformation features PDFs are observed in up to three directions. Diaplectic glass mosaicism and fluidal morphologies have been documented in Tuchscherer *et al.* (2004), also in the Yaxcopoil-1 breccias.

The characteristic inclinations vary over a wide range, larger than expected from paleosecular variation effects (Figure 6). This could indicate magnetization components acquired over extended periods and incomplete removal of secondary magnetizations. Impact breccias are characterized by complex paleomagnetic records, associated with the magnetic mineralogy, high energy emplacement and alteration processes (Halls, 1979; Elmore and Dulin, 2007; Fairchild *et al.*, 2016).

Further analyses are needed to constrain the magnetization components in the breccias and the relations to emplacement mode. The Santa Elena polymictic breccias are highly heterogeneous, with clasts of melt, basement and carbonates in a melt rich or carbonate rich matrix. Different emplacement conditions were involved, from high temperature basal surges to fall back breccias and reworking (Stoeffler *et al.*, 2004; Tuchscherer *et al.*, 2004; Kring *et al.*, 2004; Wittmann *et al.*, 2007). The remanent magnetization is probably a thermochemical or chemical magnetization, acquired after breccia emplacement. Studies of the geomagnetic field in the Mesozoic have documented an interval of constant polarity during the Cretaceous normal polarity superchron. Recent studies have focused on the paleointensity record during the superchron and extended to the K/Pg boundary interval (Goguitchaichvili *et al.*, 2004, 2023). Studies have analyzed the relationships among the frequency of reversals, secular variation and the intensity of the magnetic field. In the period before the K/Pg boundary the reversal frequency increased to around a reversal per million years.

The studies with high resolution magnetostratigraphy at the K/Pg boundary consider the paleosecular variation changes and strength of the field, in addition to the polarity changes (Zhu *et al.*, 2003; Goguitchaichvili *et al.*, 2004).

The characteristic magnetizations with upward inclinations are carried by magnetite and Ti-poor titanomagnetites, with low-intermediate coer-

http://dx.doi.org/10.18268/BSGM2024v76n3a130224

civities and distributed 300o-600o C unblocking temperatures. Pilkington *et al.* (2004) analyzed the magnetic mineralogy of the breccia section in the Yaxcopoil-1 borehole, showing that the dominant magnetic phase is magnetite formed by low temperature <150o C alteration. The secondary magnetite is associated with quartz and clays and in fine plagioclase-diopside aggregates in the melt. This association is observed for the Fe-Ti oxides and Fe-oxyhydroxides. Rock magnetic properties indicate magnetite and Ti-poor titanomagnetites (Urrutia-Fucugauchi *et al.*, 2014). Hysteresis loops for melt-rich breccias show saturation at low applied fields indicating low coercivity magnetic minerals. In the magnetization-coercivity ratio plot samples fall in the pseudo-single and multi-domain fields. Curves of magnetic susceptibility as a function of temperature show irreversible behavior, with magnetic phases formed after heating to 700o C. Well defined Hopkinson peaks are observed between 500o and 570o C. Samples subjected to a second heating run to 700o C showed similar cooling/heating curves, with reduction of magnetic susceptibility.

The remanent magnetizations carried by the secondary magnetite are likely chemical remanent magnetizations, acquired after emplacement of the breccias. The hydrothermal activity, with hot fluids circulating through the fractured porous breccias might have resulted in secondary overprints acquired over an extended period, which accounts for the multicomponent and mixed polarity magnetizations in the Yaxcopoil-1 section (Urrutia-Fucugauchi *et al.*, 2004; Pilkington *et al.*, 2004; Velasco-Villarreal *et al.*, 2011).

5. Conclusions

Results of a study in the Santa Elena borehole are used to investigate the paleomagnetic record of the impact breccias. The impact breccias cored between 332 and 504 m depth are formed by melt, basement and carbonate clasts in carbonate-rich and melt-basement-rich matrix. Thermal and alternating field demagnetization show univectorial and two-component magnetizations, with upward inclinations and few downward inclinations. The dominantly upward magnetization inclinations in the breccia sequence are interpreted in terms of reverse polarity thermoremanent magnetizations acquired during the reverse polarity ch29r chron. Magnetic susceptibility varies from 5 to 5000 10^{-6} SI, with most between 5 to 2000 10^{-6} SI. The upper section has low susceptibilities, while the lower section shows higher susceptibilities. NRM intensity log shows similar trends, with intensities between 0 to 0.5A/m, mostly between 0 to 0.15A/m. The trends correlate with the lithological and mineralogical composition, with the textural and clasts and matrix composition, with melt and basement rich in the upper section and less abundant melt particles in the lower section.

The magnetic susceptibility and remanent magnetization intensity variations throughout the upper section suggest emplacement as a fall air deposit in relatively less turbulent conditions. The trend for magnetic susceptibility and NRM in the lower unit, clast composition and petrography suggest a high temperature gas emplacement as a basal surge deposit. Analysis of thermal and AF demagnetization vector diagrams and coercivity and unblocking temperature spectra support that the upper unit is a fallback suevite and the lower unit a high temperature basal surge.

Mineralogical and chemical analyses show hydrothermal alterations that vary with location in the crater and surroundings. This resulted in formation of secondary magnetic minerals. Additional studies are needed to analyze the secondary overprints and the magnetization acquisition mechanisms.

Acknowledgements

The study forms part of the Chicxulub and Cretaceous/Paleogene Boundary Research Program. The Santa Elena borehole was drilled as part of the Chicxulub Drilling Program. We gratefully

acknowledge Marysol Valdez, Rafael Venegas and Miguel Angel Diaz for assistance with the laboratory analyses and figures. We acknowledge the comments by the two journal reviewers and editor Dr. Leda Speziale. This is contribution IICEAC 24-06

Conflict of interest

Authors confirm that there are no known conflicts of interest.

Handling editor

Leda Sánchez Bettucci.

References

Alvarez, L.W., Alvarez, W., Asaro, F. Michel, H.V., 1980, Extraterrestrial cause for the Cretaceous-Tertiary extinction: Science, 208(4448), 1095-1108. https://doi.org/10.1126/science.208.4448.1095

Besse, J., Courtillot, V., 1991, Revised and synthetic apparent polar wander paths of the African, Eurasian, North American and Indian plates, and true polar wander since 200 Ma.: Journal of Geophysical Research: Solid Earth, 96(B3), 4029-4050. https://doi.org/10.1029/90JB01916

Bourgeois, J., Hansen, T.A., Wiberg, P.L., Kauffman, E.G., 1988, A tsunami deposit at the Cretaceous-Tertiary boundary in Texas: Science, 241(4865), 567-570. https://doi.org/10.1126/science.241.4865.567

Collins S.G., Morgan J., Barton P., Christenson G.L., Gulick S., Urrutia-Fucugauchi J., Warner M., Wünnemann K., 2008, Dynamic modeling suggests terrace zone asymmetry in the Chicxulub crater is caused by target heterogeneity: Earth and Planetary Science Letters 270(3-4), 221-230. https://doi.org/10.1016/j.epsl.2008.03.032

Cornejo-Toledo, A., Hernandez-Osuna, A., 1950, Las anomalías gravimétricas en la Cuenca Salina del istmo, planicie costera de Tabasco, Campeche y Península de Yucatán: Boletín Asociación Mexicana Geólogos Petroleros, 2, 453-460.

Dearing, J., 1999, Magnetic susceptibility, in Walden, J., Oldfield, F., Smith, J.P. (eds.), Environmental magnetism: a practical guide. Technical Guide, No. 6: London, Quaternary Research Association, 35-62.

Dunlop, D.J., 1979, On the use of Zijderveld vector diagrams in multicomponent paleomagnetic studies: Physics of the Earth and Planetary Interiors, 20(1), 12-24. https://doi.org/10.1016/0031-9201(79)90103-1

Elmore, R.D. Dulin, S., 2007, New paleomagnetic age constraints on the Decaturville impact structure and Weaubleau structure along the 38th parallel in Missouri (North America): Geophysical Research Letters, 34(13), 1-5. https://doi.org/10.1029/2007GL030113

Escobar Sánchez J.E., 2002, Características litológicas de las brechas de impacto del cráter Chicxulub (pozo UNAM-5): México, UNAM, Facultad de Ingeniería, Tesis Ingeniero geólogo, 84p.

Fairchild, L.M., Swanson-Hysell, N.L., Tikoo, S.M., 2016, A matter of minutes: Breccia dike paleomagnetism provides evidence for rapid crater modification: Geology, 44(9), 723-726. https://doi.org/10.1130/G37927.1

Goguitchaichvili, A., Alva-Valdivia, L.M., Rosas-Elguera, J., Urrutia-Fucugauchi, J., Solé, J., 2004, Absolute geomagnetic paleointensity after the Cretaceous Normal Superchron and just prior to the Cretaceous-Tertiary transition: Journal of Geophysical Research: Solid Earth, 109(B1), 1-8. https://doi.org/10.1029/2003JB002477

Goguitchaichvili, A., Morales, J., Trindade, R. Kravchinsky, V.A., 2023, Testing the Mesozoic Dipole Low in the Early Cretaceous with multispecimen paleointensities from the Paraná Flood Basalts, Southern Brazil: Cretaceous Research, 148, 105539. https://

doi.org/10.1016/j.cretres.2023.105539

Gordon R.G., Van der Voo R., 1995, Mean paleomagnetic poles for the major continents and the Pacific Plate, in Ahrens T. J. (eds.), Global Earth Physics: A handbook of physical constants. Vol. 1, Washington, D.C., American Geophysical Union, 225-239. https://doi.org/10.1029/RF001p0225

Gulick, S.P.S., Christeson, G.L., Barton, P.J., Grieve, R.A.F., Morgan, J.V., Urrutia-Fucugauchi, J., 2013, Geophysical characterization of the Chicxulub impact crater: Reviews Geophysics, 51(1), 31-52. https://doi.org/10.1002/rog.20007

Halls, H.C., 1979, The Slate islands meteorite impact crater site: a study of shock remanent magnetization: Geophysical Journal International, 59(3), 553-591. https://doi.org/10.1111/j.1365-246X.1979.tb02573.x

Hildebrand A.R., Penfield G.T., Kring D.A., Pilkington M., Camargo Z., A., Jacbosen S.B. Boynton W.V., 1991, Chicxulub Crater: A possible Cretaceous/Tertiary boundary impact crater on the Yucatán Peninsula, Mexico: Geology, 19(9), .867-871. https://doi.org/10.1130/0091-7613(1991)019<0867:CCAPCT>2.3.CO;2

Hildebrand, A.R., Pilkington, M., Ortiz-Aleman, C., Chavez, R.E., Urrutia-Fucugauchi, J., Connors, M., Graniel-Castro, Camara Zi, A., Halpenny, J.F., Niehaus, D., 1998, Mapping Chicxulub crater structure with gravity and seismic reflection data, in Graddy, M.M., Hutchinson, R., McCall, G.J.H., Rotherby, D.A., (eds.), Meteorites: Flux with Time and Impact Effects: London, Geological Society, London, Special Publications, 140, 155-176. https://doi.org/10.1144/GSL.SP.1998.140.01.12

Kirschvink, J., 1980, The least-squares line and plane and the analysis of palaeomagnetic data: Geophysical Journal International, 62(3), 699-718. https://doi.org/10.1111/j.1365-246X.1980.tb02601.x

Kring, D.A., Horz, L., Zurcher, L., Urrutia Fucugauchi, J. 2004, Impact lithologies and their emplacement in the Chicxulub impact crater: Initial results from the Chicxulub scientific drilling project, Yaxcopoil, Mexico: Meteoritics Planetary Science, 39(6), 879-897. https://doi.org/10.1111/j.1945-5100.2004.tb00936.x

Kring, D. A., Tikoo, S. M., Schmieder, M., Riller, U., Rebolledo-Vieyra, M., Simpson, S.L., Osinski, G. R., Gattacceca, J., Wittmann, A., Verhagen, C.M., Cockell, C.S., Coolen, M.J. L., Longstaffe, F. J., Gulick. S.P.S., Morgan, J.V., Bralower, T.J., Chenot, E., Christeson, G. L., Claeys, P., Ferrière, L., Gebhardt, C., Goto, K., Green, S.L., Jones, H., Lofi, J., Lowery, C.M., Ocampo, R., Perez-Cruz, L., Pickersgill, A.E., Poelchau, M.H., Rae, A.S. P., Rasmussen, C., Sato, H., Smit, J., Tomioka, N., Urrutia-Fucugauchi, J., Whalen, M.T., Xiao, L., Yamaguchi, K. E. 2020, Probing the hydrothermal system of the Chicxulub impact crater: Science Advances, 6(22), eaaz3053. https://doi.org/10.1126/sciadv. aaz3053

López Ramos, 1975, Geological summary of the Yucatán peninsula, in Nair, A.E.M., Stehli, F. (eds.), The Gulf of the Mexico and the Caribbean: Boston, MA, Springer, 257-282. https://doi.org/10.1007/978-1-4684-8535-6_7

Louzada, K.L., Weiss, B.P., Maloof, A.C., Steward, S.T., Swanson-Hysell, N.L., Soule, S.A., 2008, Paleomagnetism of Lonar impact crater, India: Earth Planetary Science Letters, 275(3-4). https://doi.org/10.1016/j.epsl2008.08.025

Melosh, J.H., 1989, Impact Cratering. A geologic process: New York, Oxford University Press, 245 p.

Morgan, J.V., Gulick, S.P. S., Bralower, T., Chenot, E., Christeson, G., Claeys, P., Cockell, Ch., Collins, G.S., Coolen, M.J.L., Ferrière, L., Gebhardt, C., Goto, K., Jones, H., Kring, D.A., Le Ber, E., Lofi, J., Long, X.,

Lowery, C., Mellett, C., Ocampo-Torres, R., Osinski, G.R. Perez-Cruz, L., Pickersgill, A., Poelchau, M., Rae, A., Rasmussen, C., Rebolledo-Vieyra, M., Riller, U., Sato, H., Schmitt, D.R., Smit, J., Tikoo, S., Tomioka, N., Urrutia-Fucugauchi, J., Whalen, M., Wittmann, A., Yamaguchi, K.E., Zylberman, W., 2016, The formation of peak rings in large impact craters: Science, 354(6314), 878–882. https://doi.org/10.1126/science.aah6561

Navarro, K.F., Urrutia-Fucugauchi, J., Villagran-Muniz, M., Sanchez-Ake, C., Pi-Puig, T., Perez-Cruz, L. Navarro-Gonzalez, R., 2020, Emission spectra of a simulated Chicxulub impact-vapor plume at the Cretaceous–Paleogene boundary: Icarus, 346, 113813. https://doi.org/10.1016/j.icarus.2020.113813

Navarro, K.F., Urrutia-Fucugauchi, J., Villagran-Muniz, M., Sánchez-Aké, C., Perez-Cruz, L. Navarro-González, R., 2021, Physical characterization of a simulated impact-vapor plume using laser ablation of Chicxulub sediments: Planetary and Space Science, 206, 105311. https://doi.org/10.1016/j.pss.2021.105311

Ogg, J.G., 2020. Geomagnetic polarity time scale, in Gradstein, F.M., Ogg, J.G., Schmitz, M.D., Ogg, G.M. (eds.)., Geologic time scale 2020: USA: Elsevier, 159-192. https://doi.org/10.1016/B978-0-12-824360-2.00005-X

Ortiz-Aleman, C., Urrutia-Fucugauchi, J., 2010, Aeromagnetic anomaly modeling of central zone structure and magnetic sources in the Chicxulub crater: Physics of the Earth Planetary Interiors., 179(3-4), 127-138. https://doi.org/10.1016/j.pepi.2010.01.007

Penfield, G., Camargo-Zanoguera, A., 1981, Definition of a major igneous zone in the central Yucatan platform with aeromagnetics and gravity, in Technical Program, Abstracts and Biographies, 51st Annual Meeting: USA, Society of Exploration Geophysicists, 37 p.

Pierazzo E. Melosh H.J. 2000, Hydrocode modeling of oblique impacts: The fate of the projectile: Meteoritics Planetary Science, 35(1), 117-130. https://doi.org/10.1111/j.1945-5100.2000.tb01979.x

Pilkington, M., Hildebrand, A.R. 2000, Three-dimensional magnetic imaging of the Chicxulub crater: Journal Geophysical Research, 105(B10), 23479-23491. https://doi.org/10.1029/2000JB900222

Pilkington, M., Ames, D.E., Hildebrand A.R., 2004, Magnetic mineralogy of the Yaxcopoil-1 core, Chicxulub: Meteoritics Planetary Science 39(6), 831-841. https://doi.org/10.1111/j.1945-5100.2004.tb00933.x

Pohl J., Poschlod K., Reimold U., Meyer C., Jacob J., 2010, Ries Crater, Germany: The Enkingen magnetic anomaly and associated drillcore SUBO 18.: Geological Society America Special Paper, 465, 141-163. https://doi.org/10.1130/2010.2465(10)

Rebolledo-Vieyra M., Urrutia-Fucugauchi, J., 2006, Magnetostratigraphy of the Cretaceous/Tertiary boundary and Early Paleocene sedimentary sequence from the Chicxulub impact crater: Earth Planets and Space, 58(suppl. 10), 1309-1314. https://doi.org/10.1186/BF03352626

Renne, P.R., Deino, A.L., Hilgen, F.J., Kuiper, K.F., Mark, D.F., Mitchell III, W.S., Morgan, L.E., Mundil, R., Smit, J., 2013, Time scales of critical events around the Cretaceous-Paleogene boundary: Science, 339(6120), 684-687. https://doi.org/10.1126/science.1230492

Schulte, P., Alegret, L., Arenillas, I., Arz, J. A. , Barton, P. J., Bown, P. R., Bralower, T. J., Christenson, G. L., Claeys, P., Cockell, C. S., Collins, G. S., Deutsch, A., Goldin, T. J., Goto, K., Grajales-Nishimura, J. M., Grieve, R. A. F., Gulick, S. P. S., Johnson, K. R., Kiessling, W., Koeberl, C., Kring, D. A., Macleod, K. G., Matsui, T., Melosh, J., Montanari, A., Morgan, J. V., Neal, C. R.,

Nichols, D. J., Norris, R. D., Pierazzo, E., Ravizza, G., Rebolledo-Vieyra, M., Reimold, W. U., Robin, E., Salge, T., Speijer, R. P., Sweet, A. R., Urrutia-Fucugauchi, J., Vajda, V., Whalen, M. T., Willumsen, P. S., 2010, The Chicxulub Asteroid Impact and Mass Extinction at the Cretaceous-Paleogene Boundary: Science, 327(5970), 1214-1218. https://doi.org/10.1126/science.1177265

Sharpton, V.L, Dalrymple, G.B., Marin, L.E., Ryder, G., Schuraytz, B.G., Urrutia-Fucugauchi, J., 1992, New links between the Chicxulub impact structure and the Cretaceous-Tertiary boundary: Nature, 359, 819-821. https://doi.org/10.1038/359819a0

Sharpton, V.L., Burke, K., Camargo-Zanoguera, A., Hall, S., Marin, L., Urrutia-Fucugauchi, J., 1993, Chicxulub multiring impact basin: Size and other characteristics derived from gravity analysis: Science, 261(5128), 1564-1567. https://doi.org/10.1126/science.261.5128.1564

Steiner, M.B., 1996, Implications of magneto-mineralogic characteristics of the Manson and Chicxulub impact rocks, in Ryder, G., Fastovsky, D., Gartner, S. (eds.), The Cretaceous-Tertiary Event and Other Catastrophes in Earth History: Geological Society America Special Paper, 307, 89-104. https://doi.org/10.1130/0-8137-2307-8.89

Stöeffler D., Artemieva N., Ivanov B.A., Hecht L., Kenkemann T., Schmitt R.T., Tagle R.A, Wittman A., 2004, Origin and emplacement of the impact formations at Chicxulub, Mexico, as revealed by the ICDP deep drilling Yaxcopoil-1 and by numerical modeling: Meteoritics & Planetary Science 39(7), 1035-1067. https://doi.org/10.1111/j.1945-5100.2004.tb01128.x

Tuchscherer, M.G., Reimold, W.U., Koeberl, C., Gibson, R.L., de Bruin, D. 2004. First petrographic results on impactites from the Yaxcopoil-1 borehole Chicxulub structure, Mexico: Meteoritics & Planetary Science, 39(6), 899-930. https://doi.org/10.1111/j.1945-5100.2004.tb00937.x

Urrutia-Fucugauchi, J., Perez-Cruz, L., 2009, Multiring-forming large bolide impacts and evolution of planetary surfaces: International Geology Review, 51(12), 1079-1102. https://doi.org/10.1080/00206810902867161

Urrutia-Fucugauchi, J., Marin, L., Sharpton, V.L., 1994, Reverse polarity magnetized melt rocks from the Cretaceous/Tertiary Chicxulub structure, Yucatán peninsula, México: Tectonophysics 237(1-2), 105-112. https://doi.org/10.1016/0040-1951(94)90161-9

Urrutia-Fucugauchi, J., Marin, L., Trejo-García. A., 1996, Initial results of the UNAM scientific drilling program on the Chicxulub impact structure: rock magnetic properties of UNAM-7 Tekax borehole: Geofísica Internacional, 35(2), 125-133. https://doi.org/10.22201/igeof.00167169p.1996.35.2.854

Urrutia-Fucugauchi, J., Soler-Arechalde, A.M., Rebolledo-Vieyra, M., Vera-Sanchez, P., 2004, Paleomagnetic and rock magnetic study of the Yaxcopoil-1 impact breccia sequence, Chicxulub impact crater (Mexico): Meteoritics & Planetary Science, 39(6), 843-856. https://doi.org/10.1111/j.1945-5100.2004.tb00934.x

Urrutia-Fucugauchi, J., Camargo-Zanoguera, A., Pérez-Cruz, L., Pérez-Cruz, G., 2011, The Chicxulub multi-ring impact crater, Yucatan carbonate platform, Gulf of Mexico: Geofísica Internacional, 50(1), 99-127.

Urrutia Fucugauchi, J., Perez Cruz, L., Campos-Arriola, S., Escobar-Sánchez, E., Velasco-Villarreal, M., 2014, Magnetic susceptibility logging of Chicxulub proximal impact breccias in the Santa Elena borehole – Breccia characterization and ejecta blanket. Studia Geophysica et Geodaetica 58, 100-120. https://doi.org/10.1007/s11200-013-0803-0

Urrutia-Fucugauchi, J., Arellano-Catalán, O., Pérez-Cruz, L., Romero, I.A., 2022, Chicxulub crater joint gravity and magnetic

anomaly analysis: Structure, asymmetries, impact trajectory and target structures. Pure and Applied Geophysics, 179(8), 2735-2756. https://doi.org/10.1007/s00024-022-03074-0

Velasco-Villarreal, M., Urrutia-Fucugauchi, J., Rebolledo-Vieyra, M., Perez-Cruz, L., 2011, Paleomagnetism of impact breccias from the Chicxulub crater – implications for ejecta emplacement and hydrothermal processes: Physics Earth and Planetary Interiors 186 (3-4), 154-171. https://doi.org/10.1016/j.pepi.2011.04.003

Wittmann, A., Kenkmann, T., Hecht, L., Stöffler, D., 2007, Reconstruction of the Chicxulub ejecta plume from its deposits in drill core Yaxcopoil-1: Geological Society America Bulletin, 119(9-10) 1151-1167. https://doi.org/10.1130/B26116.1

Yokoyama, E., Trindade, R.I.F.D., Lana, C., Souza Filho, C.R.D., Baratoux, D., Marangoni, Y.R. Tohver, E., 2012, Magnetic fabric of Araguainha complex impact structure (Central Brazil): Implications for deformation mechanisms and central uplift formation: Earth and Planetary Science Letters, 331-332, 347-359. https://doi.org/10.1016/j.epsl.2012.01.00